J|A|C|S ARTICLES

Published on Web 05/19/2010

Molecular Recognition at the Membrane−Water Interface: Controlling Integral Peptide Helices by Off-Membrane Nucleobase Pairing

Philipp Erik Schneggenburger, Stefan Müllar, Brigitte Worbs, Claudia Steinem, and Ulf Diederichsen*

Institute for Organic and Biomolecular Chemistry, Georg-August-University Göttingen, 37077 Göttingen, Germany

Received January 24, 2010; E-mail: udieder@gwdg.de

Abstract: The aggregation and organization of membrane proteins and transmembrane peptides is related to the interacting molecular species itself and strongly depends on the lipid environment. Because of the complexity and dynamics of these interactions, they are often hardly traceable and nearly impossible to predict. For this reason, peptide model systems are a valuable tool in studying membrane associated processes since they are synthetically accessible and can be readily modified. To control and study the aggregation of peptide transmembrane domains (TMDs) the interacting interfaces of the TMDs themselves can be altered. A second less extensively studied approach targets the TMD assembly by using interaction and recognition of domains at the membrane outside as frequently found in the membrane protein interplay and protein assembly. In the present study, double helical transmembrane domains were designed and synthesized on the basis of a recently reported D,L-alternating peptide pore motif derived from gramicidin A. The highly hydrophobic and aromatic transmembrane peptide was covalently functionalized with a short peptide nucleic acid (PNA) used as specific outer-membrane recognition unit. The PNA sequences were chosen with high polarity to ensure localization within the aqueous phase. To estimate the impact of the membrane adjacent recognition on the TMD assembly by Förster resonance energy transfer (FRET), fluorescence probes were covalently attached to the side chains of the membrane spanning peptide helices. Dimerization of the TMD-peptide/PNA conjugates within unilamellar lipid vesicles was observed. The dimer/monomer ratio of TMDs can be controlled by temperature variation.

Introduction

Integral membrane proteins represent about 20−30% of all proteins in sequenced genomes.[1] While certain membrane proteins are functional as monomers, others need to assemble into oligomeric structures to carry out their biological role. These membrane protein oligomers form ion channels and pore structures via arrangement of transmembrane domains and are often involved in key cellular processes such as protein translocation and respiration.[2] Forces directing and stabilizing membrane protein oligomerization have been identified in several experimental studies using model systems of single spanning transmembrane peptide helices. Sequences like the Gly-xxx-Gly motif (x = any other amino acid residue) inducing a helix topology for proper interaction or single residue electrostatic recognition promote the ability of individual transmembrane helix surfaces to adopt close contact sides.[3,4] Additionally, interhelical hydrogen bonds between polar amino acid residues may further stabilize helix−helix contacts.[5−11] Nevertheless, this direct approach of subunit interactions via charges or fit of transmembrane helix topologies does not provide the flexibility many protein assemblies require.[12] The presence of charges in the membrane might impose difficulties in constructing ion selective pores. In case of the nicotinic acetylcholine receptor (AChR), the interaction between the luminal, N-terminal domains is suggested as initial step in the association of the subunits.[12] According to this model, the recognition of the N-terminal domains and interaction at the luminal membrane side facilitate the subsequent interaction and assembly of transmembrane as well as cytoplasmic domains from different subunits of the AChR machinery.

To our knowledge, very little is reported on model systems dealing with this specific high-affinity interaction at the membrane surface providing an organizing and assembling effect on structured transmembrane domains. Existing model

(1) Wallin, E.; v. Heijne, G. *Protein Sci.* **1998**, *7*, 1029–1038.
(2) Rath, A.; Deber, C. M. *Proteins* **2008**, *70*, 786–793.
(3) Unterreitmeier, S.; Fuchs, A.; Schäffler, T.; Heym, R. G.; Frishman, D.; Langosch, D. *J. Mol. Biol.* **2007**, *374*, 705–718.
(4) Choma, C.; Gratkowski, H.; Lear, J. D.; DeGrado, W. F. *Nat. Struct. Biol.* **2000**, *7*, 161–166.
(5) Senes, A.; Engel, D. E.; DeGrado, W. F. *Curr. Opin. Struct. Biol.* **2004**, *14*, 465–479.
(6) Walters, R. F.; DeGrado, W. F. *Proc. Natl. Acad. Sci. U.S.A.* **2006**, *103*, 13658–13663.
(7) Dawson, J. P.; Weinger, J. S.; Engelman, D. M. *J. Mol. Biol.* **2002**, *316*, 799–805.
(8) North, B.; Christian, L.; Fu Stowell, X.; Lear, J. D.; Saven, J. G.; DeGrado, W. F. *J. Mol. Biol.* **2006**, *359*, 930–939.
(9) Rath, A.; Tulumello, D. V.; Deber, C. M. *Biochemistry* **2009**, *48*, 3036–3045.
(10) Lee, J.; Im, W. *J. Am. Chem. Soc.* **2008**, *130*, 6456–6462.
(11) Yano, Y.; Matsuzaki, M. *Biochemistry* **2006**, *45*, 3370–3378.
(12) Hall, Z. W. *Trends Cell. Biol.* **1992**, *2*, 66–68.

10.1021/ja1006349

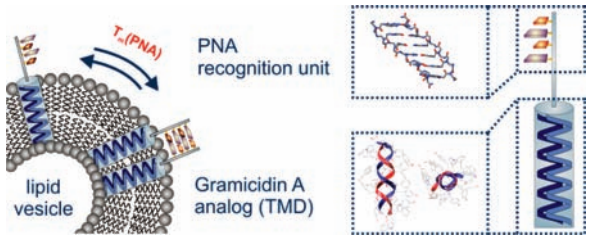

Figure 1. Concept and structural design of outer-membrane PNA nucleobase recognition with impact on the aggregation of transmembrane domains (TMDs), controllable by the applied temperature.[17,18]

systems either focus on the molecular recognition of species solely anchored to the membrane surface or on the direct interaction of transmembrane helices.[9,13−16] Since the single steps of the described recognition and assembling processes are located in environments of opposing polarities shielded from each other by the lipid head groups, it is challenging to create peptide model systems operating at this interface and being affected by the membrane properties like lipid bilayer composition, hydrophobic matching, and membrane fluctuation.

A solid phase peptide synthesis approach was selected to obtain a model system that does not mimic a certain domain of a native protein species but provides a process analogy to face general questions concerning the effect of environmental properties on in-membrane helix assembly that is induced by a preorganization at the membrane's adjacent water layers.

Herein, the design and synthesis of an artificial peptide conjugate is described containing a β-helical membrane spanning domain that is structurally derived from the D,L-alternating gramicidin A pore motif.[17] This domain was covalently attached to a peptide nucleic acid (PNA) recognition moiety by a linker capable of penetrating the lipid headgroup region. Dimerization of the TMDs within the lipid environment of unilamellar vesicles based on temperature dependent PNA recognition at the membrane outside was studied providing proof-of-concept for the designed system (Figure 1). The recognition and assembling process of the transmembrane helices is, thereby, followed within phospholipid vesicles by means of Förster resonance energy transfer (FRET) experiments. With respect to the applied technique, fluorophores were attached to the N-terminal side chain of the transmembrane segments.

A reliable and reproducible peptide model on basis of the presented prototype allows addressing the question why nature uses the mode of protein interaction that was described above instead of direct in-membrane recognition that has been extensively studied and was ascribed to a variety of different driving forces.[2,10,19] It can be assumed that the influence, for example, hydrophobic matching or the directing effect of lipid domain formation, appears considerably different in case of a recognition at the membrane's outside. The use of PNAs is not limited to dimerization, although it is the simplest case, and it is, furthermore, suited to evaluate dynamical changes if applied to interacting transmembrane helices, for example, by adjusting the directing effect via variation of the respective linker length.[20,21] This would likewise lead to an enhanced understanding why the described process of an initial interaction and recognition prior to transmembrane helix assembly is favored in several protein assemblies. Furthermore, the idea of applying structured PNA/TMD conjugates at the membrane−water interface is generally applicable to study reversible interaction processes at membrane surfaces, for example, by modulating membrane associated substrate conversion pathways that are mediated by adhesively bound enzymes.

Experimental Section

The solid phase synthesis of a peptide model system as described above required the thorough design of the transmembrane domain with respect to its invariability, geometry concordant with hydrophobic matching, and its orientation within the membrane. Single transmembrane domains were synthesized (Supporting Information) and studied applying CD and fluorescence spectroscopy. Prior to synthesis of the entire TMD/PNA constructs, the proper choice of stability, selectivity, and strand orientation of the PNA double strand recognition moiety was analyzed by UV spectroscopy determining oligomer length and sequence. The initial studies were followed by orthogonal functionalization of the TMD with respective FRET probes and a PNA recognition unit coupled by polyethylene glycol (PEG) linker. The donor/acceptor labeled constructs were applied to the recognition process by incorporation into unilamellar lipid vesicles and FRET assays.

Preparation of Lipid−Peptide Complexes. Large unilamellar vesicles (LUVs) of 1,2-dilauroyl-*sn*-glycero-3-phosphocholine (DLPC) were prepared in phosphate buffer (1 mM NaH_2PO_4/Na_2HPO_4, pH = 7.0) following methods of MacDonald et al.[28] For CD spectroscopy, DLPC dissolved in $CHCl_3$ (10 mg/mL) and the peptides dissolved in MeOH were mixed yielding a solution of $CHCl_3$/MeOH (1/1, v/v). Concentrations of peptide stocks were determined by UV absorption. Removing the solvents in a nitrogen stream at temperatures above the lipid main phase transition temperature of DLPC ($t_m = -2.1$ °C)[23] produced an almost clear lipid/peptide film at the test tube walls. After removing of residual solvent under reduced pressure for 12 h at $T > t_m$, the lipid films were rehydrated with buffer solution. After 1 h of incubation at $T > t_m$, the hydrated lipid films were vortexed several times for 30 s with subsequent incubation for 5 min (5 cycles). The milky suspensions were extruded 25 times through a polycarbonate membrane (100 nm nominal pore size) using a miniextruder (Liposofast, Avestin, Ottawa, Canada) to produce an almost clear vesicle suspension. Subsequently, the vesicle suspensions were deposited in precision cells (Quartz Suprasil, Hellma, Mühlheim, Germany). In case of fluorescence spectroscopy (FRET analysis), DLPC dissolved in $CHCl_3$ (40 mg/mL) and peptides dissolved in MeOH (concentration estimated via UV absorption) were mixed under occasional swirling in the following order: (i) DLPC, (ii) donor fluorophore labeled species (**15**, **18**), (iii) acceptor fluorophore species (**16**, **19**), (iv) nonlabeled species (**17**, **20**). The mixtures were heated to 40 °C prior to solvent removal in the nitrogen stream and treated as

(13) Marsden, H. R.; Elbers, N. A.; Bomans, P. H. H.; Sommerdijk, N. A. J. M.; Kros, A. *Angew. Chem.* **2009**, *121*, 2366–2369. *Angew. Chem., Int. Ed.* **2009**, *48*, 2330−2333.
(14) Kashiwada, A.; Matsuda, K.; Mizuno, T.; Tanaka, T. *Chem.—Eur. J.* **2008**, *14*, 7343–7350.
(15) Stengel, G.; Zahn, R. *J. Am. Chem. Soc.* **2007**, *129*, 9584–9585.
(16) Chan, Y.-H. M.; van Lengerich, B.; Boxer, S. G. *Proc. Natl. Acad. Sci. U.S.A.* **2009**, *106*, 979–984.
(17) Küsel, A.; Khattari, Z.; Schneggenburger, P. E.; Banerjee, A.; Salditt, T.; Diederichsen, U. *ChemPhysChem* **2007**, *8*, 2336–2343.
(18) Rasmussen, H.; Kastrup, J. S.; Nielsen, J. N.; Nielsen, J. M.; Nielsen, P. E. *Nat. Struct. Biol.* **1997**, *4*, 98–101.
(19) Tiwari-Woodruff, S. K.; Schulteis, C. T.; Mock, A. F.; Papazian, D. M. *Biophys. J.* **1997**, *72*, 1489–1500.
(20) Krishnan-Ghosh, Y.; Stephens, E.; Balasubramanian, S. *J. Am. Chem. Soc.* **2004**, *126*, 5944–5945.
(21) Wittung, P.; Nielsen, P.; Nordén, B. *J. Am. Chem. Soc.* **1997**, *119*, 3189–3190.
(22) MacDonald, R. C.; MacDonald, R. I.; Menco, B. P. M.; Takeshita, K.; Subbarao, N. K.; Hu, L. *Biochim. Biophys. Acta* **1991**, *1061*, 297–303.
(23) Oliynyk, V.; Jäger, M.; Heimburg, T.; Buckin, V.; Kaatze, U. *Biophys. Chem.* **2008**, *134*, 168–177.

described above. The resulting peptide lipid complexes were kept at 40 °C until adjusting to room temperature was allowed prior to extrusion.

FRET Analysis. Fluorescence spectra were obtained with a JASCO FP 5600 fluorescence spectrometer (Gross-Umstadt, Germany) under temperature control using a thermostat (Model 1162A, VWR International, Darmstadt, Germany). Fluorescence was excited at 485 nm with a detection of the fluorescence emission between 495 and 700 nm. The excitation and emission bandwidths were set to 3 nm, the data pitch was 1 nm, and the response time was adjusted to 0.2 s. Oligomers **15** and **18** were equipped with 7-nitro-2-1,3-benzoxadiazol-4-yl (NBD) as donor (D) fluorophore and 5(6)-carboxytetramethylrhodamine (TAMRA) served as acceptor (A) in oligomers **16** and **19**. For temperature dependent measurements at equimolar concentrations of either peptide/PNA conjugates **15**/**16** or the control species **18**/**19**, the total peptide concentration was adjusted to 5.5 μM. The temperature was varied between 10 and 80 °C with $\Delta T = 10$ °C, using a 5 min cycle for each thermal equilibration. The data shown in Figure 5 were recorded at a P/L-ratio of 1/1000 in DLPC LUVs. In case of the concentration dependent FRET-analysis (Figure 6), the concentration of peptide **15**, as well as the total peptide concentration, was kept constant using the nonlabeled peptide **17**. The concentration of peptide **15** was adjusted to 2.75 μM, while varying the concentration of **16** from 0.00 to 2.20 μM (DLPC LUVs, P/L = 1/1000). After extrusion of the lipid vesicles, the fluorescence emission of the sample was measured at 20 °C. After heating and equilibrating at 60 °C, the sample was measured again, then cooled and reequilibrated at 20 °C to check for reversibility. For plotting the donor fluorescence as a function of temperature or the mole fraction of the acceptor peptide, the fluorescence intensity at 530 nm was displayed. For the control experiment using fluorophore labeled transmembrane domains **18**−**20** lacking the PNA recognition moiety, an identical sample preparation and data treatment was applied. For the plots of the control, four data sets were averaged (Supporting Information).

Theoretical Treatment of the FRET Data. The dependence of the fluorescence emission intensity of donor (NBD)-labeled peptides on the mole fraction of acceptor (TAMRA)-labeled peptides in a lipid bilayer enables the determination of the number of subunits in the peptide assembly.[24] This model is based on four assumptions: (i) labeling does not influence the aggregation of the peptides, (ii) all peptides are located in the lipid bilayer, (iii) the interaction of the peptides is random, and (iv) one acceptor is capable of quenching all donors within one aggregate.[25] With a random number of donors and acceptors in the vesicles, the total number of quenched (N_Q) and nonquenched donors (N_D) follows a binomial distribution. The recorded relative fluorescence (F/F_0) is, thus, related to N_Q and N_D (eq 1):

$$\frac{F}{F_0} = 1 - \left(1 - \frac{f_Q}{f_D}\right)\frac{N_Q}{N_D} \tag{1}$$

where F is the fluorescence in the presence of the acceptor labeled peptides and F_0 that in its absence, f_D is the molar fluorescence of nonquenched donor D, and f_Q that of quenched donor. With $\chi_A + \chi_D + \chi_u = 1$, where χ_A denotes the mole fraction of the acceptor peptide, χ_D the one of the donor and χ_u that of the nonlabeled peptide, and the assumption of a monomer−oligomer equilibrium, the following expression can be written to describe a monomer−dimer equilibrium (eq 2):

$$\frac{F}{F_0} = m\left(\frac{F}{F_0}\right)_m + (1 - m)\left(1 - \chi_D\frac{\chi_A}{\chi_D}\right) \tag{2}$$

where m is the peptide fraction of the monomeric state and $1 - m$ that of the dimeric state. The equation for a monomer−trimer equilibrium reads (eq 3):

$$\frac{F}{F_0} = m\left(\frac{F}{F_0}\right)_m + (1 - m)\left[1 - \chi_D^2\left(\frac{2}{\chi_D}\right)\left(\frac{\chi_A}{\chi_D}\right) - \left(\frac{\chi_A}{\chi_D}\right)^2\right] \tag{3}$$

The dissociation constant K_D is defined as (eq 4):

$$K_D = \frac{(m\chi_P)^n}{(1 - m)\chi_P/n} \tag{4}$$

where χ_P is the lipid-to-peptide ratio and n the number of species in the oligomer. K_D is expressed in units of peptide/lipid mole fraction (MF). For the presented simulated plots (Figure 6 C,D), the Förster radius was set to $R_0 = 5.1$ nm as estimated in previous experiments for the NBD/TAMRA-pair.[25]

By taking the Förster radius and the geometry of the peptide helices with an approximate helix length of 26 Å and a diameter of 6 Å into account, a fluorescence transfer efficiency of $E = 99.9\%$ is calculated assuming a parallel assembly of the helices. An antiparallel peptide assembly would yield $E = 97.9\%$.[26] As in both cases, for parallel as well as for the antiparallel configuration, the transfer efficiencies are very high, the two different scenarios cannot be distinguished. Using this approximation, the statistical occurrence of FRET in a vesicle without the formation of aggregates was taken into account (eq 5):

$$\left(\frac{F}{F_0}\right)_m = A_1 \exp\left(-k_1\chi_A\frac{N_0}{A}R_0^2\right) + A_2 \exp\left(-k_2\chi_A\frac{N_0}{A}R_0^2\right) \tag{5}$$

where A_1, A_2, k_1, k_2 are constants, N_0 is the total number of peptides, and A the area of one vesicle.[28] The constants are chosen for $R_e/R_0 = 0$.[28] R_e is the radius of closest approach. The area of a DLPC lipid was assumed to be 0.63 nm^2.[29]

Results and Discussion

The design of the construct used for studying the dimerization of transmembrane helices induced by base pair recognition of attached outer-membrane oligomers required a conformationally stable and uniform helix motif. The TMDs were, thus, based on a recently reported homodimer peptide analogue of the natural antibiotic gramicidin A (gA).[30−32] As indicated by X-ray crystallography, the peptide H-(Y$\underline{\text{Y}}$)$_4$K-OH (**1**) with D,L-alternating configuration exhibits an antiparallel, double helical motif providing a water mediated hydrogen bonding network of β-helical tubes.[30] In a β-helix, all peptide side chains are oriented to the helix outside, and the presented motif provides helices with a periodicity of 5.6 residues. The peptide H-($\underline{\text{F}}$Y)$_5$$\underline{\text{W}}$W-OH (**2**) likewise adopts this homodimeric $\beta^{5.6}$-helical structure

(24) Adair, B. D.; Engelman, D. M. *Biochemistry* **1994**, *33*, 5539–5544.
(25) Naarmann, N.; Bilgiçer, B.; Kumar, K.; Steinem, C. *Biochemistry* **2005**, *44*, 5188–5195.
(26) Naarmann, N.; Bilgiçer, B.; Meng, H.; Kumar, K.; Steinem, C. *Angew. Chem.* **2006**, *118*, 2650–2653. *Angew. Chem., Int. Ed.* **2006**, *45*, 2588−2591.
(27) You, M.; Li, E.; Wimley, W. C.; Hristova, K. *Anal. Biochem.* **2005**, *340*, 154–164.
(28) Wolber, P. K.; Hudson, B. S. *Biophys. J.* **1979**, *28*, 197–210.
(29) Kučerka, N.; Liu, Y.; Chu, N.; Petrache, H. I.; Tristam-Nagle, S.; Nagle, J. F. *Biophys. J.* **2005**, *88*, 2626–2637.
(30) Alexopoulos, E.; Küsel, A.; Sheldrick, G. M.; Diederichsen, U.; Usón, I. *Acta Crystallogr., Sect. D: Biol. Crystallogr.* **2004**, *60*, 1971–1980.
(31) Andersen, O. S. *Annu. Rev. Physiol.* **1984**, *46*, 531–548.
(32) Kelkar, D. A.; Chattopadhyay, A. *Biochim. Biophys. Acta* **2007**, *1768*, 2011–2025.

and can be incorporated as TMD into lipid bilayers.[17] This membrane active pore motif has been revealed to span the membrane hydrophobic core with the tryptophan residues anchoring at the lipid headgroup interfacial region of DLPC (12:0) and 1,2-dimyristoyl-*sn*-glycero-3-phosphocholine (DMPC, 14:0) peptide/lipid complexes.[17,33]

Conformational Restricted Hairpin Linked $\beta^{5.6}$-Helix. As known from gA, the $\beta^{5.6}$-helix of D/L-alternating peptides exists in an equilibrium with the $\beta^{6.3}$-form. As the $\beta^{5.6}$-double helical arrangement spans the entire hydrophobic lipid bilayer core, the $\beta^{6.3}$-single channel is capable of penetrating one single leaflet of the membrane while a lateral bilayer dynamic enables a head-to-head junction assembly that constitutes the channel conformer. Several functional, linked channel forms ($\beta^{6.3}$-helical) derived from gA have been reported, for example, using special amino acid building blocks or tartaric acid residues.[34−36] To preserve the $\beta^{5.6}$-helical pore conformation spanning the entire hydrophobic bilayer core and to further exclude a monomer−dimer equilibrium, the transmembrane domain H-(FY)$_5$WW-GKPG-(FY)$_5$WW-OH (**3**) was introduced. This peptide structure contains a loop region that covalently links the antiparallel oriented peptide strands in the double helical conformation. In this case, the reverse turn with the sequence GKPG emerged to be the appropriate motif with respect to retaining the $\beta^{5.6}$-helical pore conformation.[37] Flanking tryptophan residues are implemented in order to ensure a membrane spanning orientation via interfacial anchoring at the glycerol carbonyl sites (beneath the lipid headgroup) on both sides of the membrane.[38] In addition to positioning of the helix perpendicular to the membrane surface, tryptophan residues are known to promote a lateral interaction of membrane spanning peptide helices.[39,40] With the applied design, we have taken advantage of the lateral aggregation potential that facilitates close contact within the helix assembly. For this reason, transmembrane helices are designed to be directed via PNA recognition in the water phase adopting a side chain mediated parallel orientation within the hydrophobic bilayer core.

Circular dichroism (CD) analysis of the hairpin structure **3** within large unilamellar DLPC vesicles showed the typical characteristics of an antiparallel $\beta^{5.6}$-helical double strand with maxima at 228 and 205 nm and a negative Cotton effect below 200 nm.[41,42] The decrease in molar ellipticity compared to homodimer **2** can be assigned to missing charges due to the reverse turn modification substituting the peptide termini that are normally charged under physiological conditions (Figure 2).[33] This hypothesis was validated by CD spectra comparison of oligomer **2** with terminal noncharged *N*-acyl and/or *C*-amide functionalized homodimers H-(FY)$_5$WW-NH$_2$ (**4**) and Ac-(FY)$_5$WW-NH$_2$ (**5**). A correlation of a lower helical content with lacking terminal Coulomb interactions was observed. Thus, charged termini appear to be relevant for intramolecular terminal interaction between both strands of the nonconnected side of the hairpin (charge compensation) and for an interaction with the lipid headgroup interface (polarity). Therefore, the C- and N-terminus are not addressable for further functionalization of the TMD with fluorophore labels.

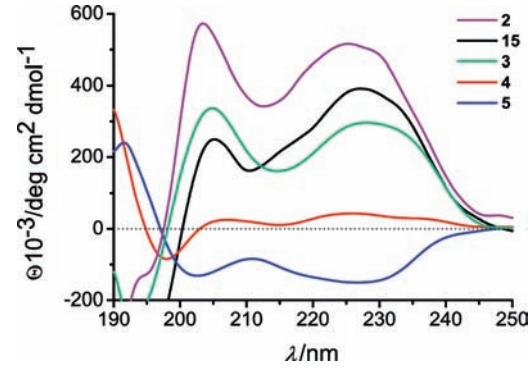

Figure 2. CD spectra of the homodimeric transmembrane domains H-(FY)$_5$WW-OH (**2**), H-(FY)$_5$WW-NH$_2$ (**4**), and Ac-(FY)$_5$WW-NH$_2$ (**5**) varying in constitution of the peptide termini, the hairpin transmembrane domain H-(FY)$_5$WW-GKPG-(FY)$_5$WW-OH (**3**), and the fluorophore (NBD) labeled as well as PNA functionalized system H-(K(NBD)Y(FY)$_4$WW-GK(C$_2$H$_4$O)$_2$-gcgtggKK-H)PG-(FY)$_5$WW-OH (**15**) (see below) reconstituted in DLPC vesicles.

Design of the PNA Recognition System. Aggregation analysis of the transmembrane domain by means of FRET required functionalization of the double helical loop structure **3** with fluorophores NBD or TAMRA. Being aware of conformational restrictions by attaching the fluorophores to the terminal ends and the indispensability of free peptide termini, a lysine residue was introduced as N-terminal amino acid facilitating a side chain attachment of the fluorophores as amides (Scheme 1). Aminoethylglycine (aeg)-PNA was selected as outer-membrane recognition motif since it is synthetically compatible with Fmoc-solid phase peptide synthesis (SPPS) that was likewise applied for the synthesis of the transmembrane domain. Furthermore, PNA allows duplex formation also with parallel strand orientation and provides an appropriate duplex stability, selectivity, and polarity as desired for the model recognition system.[43,44] The PNA double strand should be placed in close proximity to the membrane surface with a reasonable short PNA duplex not exceeding the TMD length of about 26 Å in order to allow for application of highly aligned multilamellar membrane stacks in future experiments.[45−47] Attachment of the PNA recognition unit to the TMD was conducted at the lysine side chain within the loop region. A diethylene glycol amino acid building block (Fmoc-HN-(C$_2$H$_4$O)$_2$CH$_2$-COOH) was used to link the water-soluble PNA oligomer and the highly hydrophobic transmembrane domain. This linker is well suited to penetrate the lipid head groups that separate the regimes of opposing polarity (Scheme 1). A temperature induced transition from duplex to single strand PNA was supposed to serve as a reversible trigger

(33) Schneggenburger, P. E.; Beerlink, A.; Worbs, B.; Salditt, T.; Diederichsen, U. *ChemPhysChem* **2009**, *10*, 1567–1576.
(34) Essen, L.-O.; Koert, U. *Annu. Rep. Prog. Chem., Sect. C: Phys. Chem.* **2008**, *104*, 165–188.
(35) Xie, X.; Al-Momani, L.; Rei*β*, P.; Griesinger, C.; Koert, U. *FEBS J.* **2005**, *272*, 975–986.
(36) Stankovic, C. J.; Heinemann, S. H.; Schreiber, S. L. *J. Am. Chem. Soc.* **1990**, *112*, 3702–3704.
(37) Sastry, M.; Brown, C.; Wagner, G.; Clark, T. D *J. Am. Chem. Soc.* **2006**, *128*, 10650–10651.
(38) De Planque, M. R. R.; Killian, J. A. *Mol. Membr. Biol.* **2003**, *20*, 271–284.
(39) Ridder, A.; Skupjen, P.; Unterreitmeier, S.; Langosch, D. *J. Mol. Biol.* **2005**, *354*, 894–902.
(40) Adamian, L.; Liang, J. *J. Mol. Biol.* **2001**, *311*, 891–907.
(41) Koeppe II, R. E.; Andersen, O. S. *Annu. Rev. Biophys. Biomol. Struct.* **1996**, *25*, 231–258.
(42) Chen, Y.; Wallace, B. A. *Eur. Biophys. J.* **1997**, *26*, 299–306.
(43) Nielsen, P. E.; Egholm, M.; Berg, R. H.; Buchardt, O. *Science* **1991**, *254*, 1497–1500.
(44) Nielsen, P. E.; Egholm, M. *Peptide Nucleic Acids-Protocols and Applications*, Horizon Scientific Press, Wymondham, 1999.
(45) Salditt, T. *Curr. Opin. Struct. Biol.* **2003**, *13*, 467–478.
(46) Mennicke, U.; Salditt, T. *Langmuir* **2002**, *18*, 8172–8177.
(47) Fahsel, S.; Pospiech, E.-M.; Zein, M.; Hazlet, T. L.; Gratton, E.; Winter, R. *Biophys. J.* **2002**, *83*, 334–344.

Scheme 1. Exemplarily SPPS of TMD/PNA Conjugate **15** with NBD-Donor Labeling

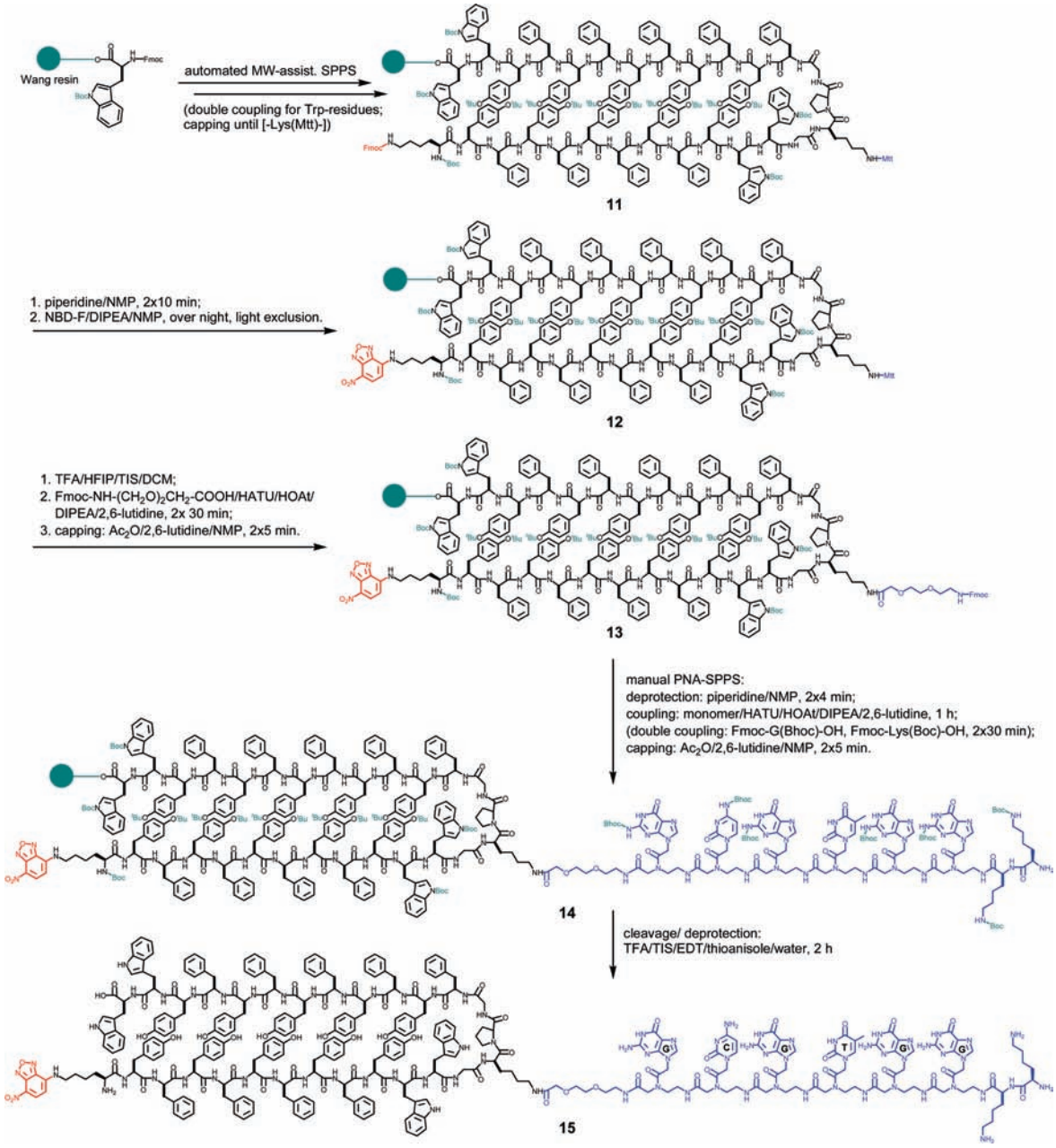

for the assembly and disassembly of the transmembrane domains. Thus, the stability of the PNA double strand, that is, its melting temperature T_m, was chosen to be settled well above the lipid main phase transition temperature t_m to ensure that the bilayers composed of DLPC ($t_m = -2.1$ °C)[23] or DMPC ($t_m = 23.6$ °C)[48] are continuously adopting the liquid L_α-phase unaffected by the temperature dependent pairing and melting of the PNA double strand. Summarizing, the PNA moiety should be rather short in sequence regarding its applicability for different substrates, further being guanine-cytosine rich to reach the aspired melting transition interval of 30−55 °C. Additionally, the PNA strands should contain a sufficient number of base pairs to still enable a selective recognition process avoiding higher ordered aggregation like guanine tetrad formation.[49]

Several short PNA sequences lacking the TMD were synthesized in order to evaluate the differences in stability between parallel and antiparallel strand orientation of respective double strands and to further estimate the appropriate length with respect to requirements mentioned before. PNA octamers H-$(Gly)_3$-cgcttacc-$(Lys)_2$-NH_2 (**6**) and H-$(Gly)_3$-ggtaagcg-$(Lys)_2$-NH_2 (**7**) formed an antiparallel double strand ($T_m = 72.4$ °C), whereas parallel strand orientation ($T_m = 72.7$ °C) was provided with PNA **6** and H-$(Gly)_3$-gcgaatgg-$(Lys)_2$-NH_2 (**8**). The stabilities of PNA octamers were too high to trigger temperature dependent disassembly. Preferentially, PNA aggregates with parallel strand orientation were investigated having both TMDs

(48) Heimburg, T. *Thermal Biophysics of Membranes*, Wiley-VCH, Weinheim, 2007.

(49) Datta, B.; Bier, M. E.; Roy, S.; Armitage, B. A. *J. Am. Chem. Soc.* **2005**, *127*, 4199–4207.

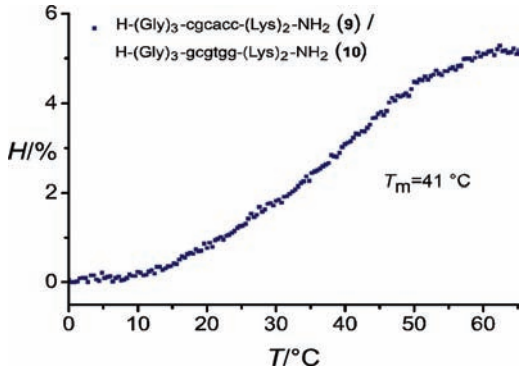

Figure 3. Melting curve obtained by UV spectroscopy for the equimolar mixture of PNA hexamers **9** and **10** (10 mM NaH_2PO_4/Na_2HPO_4, 100 mM NaCl, pH = 7.0) used as recognition unit with T_m = 41 °C.

aligned and attached at the respective C-terminal end. UV analyses of the duplex formed by parallel oriented hexamers H-$(Gly)_3$-cgcacc-$(Lys)_2$-NH_2 (**9**) and H-$(Gly)_3$-gcgtgg-$(Lys)_2$-NH_2 (**10**) revealed a melting temperature of 41 °C (Figure 3). This stability is in the appropriate range for serving as recognition device within the envisioned model system. This T_m is high enough to ensure standard phospholipids to remain in the fluid membrane state, and is still applicable as trigger parameter. For the melting experiments, the PNA sequences were investigated without the TMD attached, since the TMD/PNA constructs were insufficiently soluble in aqueous media requiring the lipid environment for solubilization of the hydrophobic transmembrane segment.

Synthesis of TMD/PNA Constructs. Preparation of the resin bound, fully protected transmembrane hairpin was provided by automated microwave-assisted Fmoc-SPPS. Double coupling was performed for the tryptophan residues. Capping of nonreacted free amine functionalities was only performed until incorporation of the Mtt-protected lysine residue in order to avoid acylation of the secondary amine functionality.[50] Lysine side chains were orthogonally protected to enable attachment of the fluorescence probes at the side chain of the N-terminal lysine residue as well as PNA functionalization at the lysine residue of the turn region in the following step. Therefore, the Fmoc- and the 4-methyltrityl (Mtt)-protection groups were applied during the assembly of the transmembrane domain allowing regioselective diversification (Scheme 1). As protecting group pattern of the terminal lysine residue, Fmoc-protection at the side chain and Boc-protection at the N-terminus were used. Accomplishing the automated synthesis of resin bound TMD **11** followed by Fmoc-deprotection, the FRET probe 4-fluoro-7-nitrobenzofurazan (NBD-F) was coupled to the side chain amino functionality of the N-terminal lysine residue yielding peptide **12** (Scheme 1). This was followed by selective deprotection of the highly acid labile lysine Mtt-group in the GKPG-turn, at which the diethylene glycol amino acid was subsequently attached. For elongation of the resin bound TMD domain **13** with the PNA sequence via manual SPPS (Fmoc/Bhoc-strategy), some precautions had to be taken according to deprotection and capping cycles. To suppress base-catalyzed transamidation rearrangement by the nascent primary amine that would either lead to base deletion or sequence termination,[42] the deprotection times were kept short and double couplings with diminished coupling times were performed for the Fmoc-aeg-G(Bhoc)-monomer; for this building block, side reactions were most prominent. Self-capping by 'acetyl-nucleobase' species during the neutralization/deprotection step was avoided by NMP/DIPEA washing introduced after the capping cycle.[51]

At the N-terminal end of the PNA sequence, two lysine residues were attached to give construct **14**. They were introduced for enhancement of the segment polarity and should ensure localization within the membrane adjacent water layers. Finally, the fluorophore labeled constructs H-(K(NBD)Y(FY)$_4$-WW-GK$(C_2H_4O)_2$-gcgtggKK-H)PG-$(FY)_5$WW-OH (**15**) and H-(K(TAMRA)Y(FY)$_4$WW-GK$(C_2H_4O)_2$-cgcaccKK-H)PG-$(FY)_5$WW-OH (**16**) were obtained being complementary in their PNA nucleobase sequences. Purification was performed via dialysis in combination with RP-HPLC using a C4 stationary phase. Structural integrity of the oligomers was proven by high-resolution mass spectrometry. Details regarding synthesis, purification, and characterization are given in the Supporting Information.

In addition to the PNA sequence complementary constructs **15** and **16** carrying the donor and acceptor fluorescence probe, respectively, a third construct **17** with identical PNA sequence compared to the acceptor-species **16** but lacking the fluorescence label was synthesized. The nonlabeled species **17** was acylated at the side chain position of the terminal lysine of the transmembrane domain (Figure 4). It was used to ensure a constant total peptide concentration and, therefore, a constant peptide-to-lipid ratio throughout the mixing experiments within the lipid bilayer.

The $\beta^{5.6}$-helical TMD structure of peptide **15** was exemplarily verified by CD spectroscopy after incorporation in DLPC vesicles (Figure 2). The CD spectrum still revealed high $\beta^{5.6}$-helix propensity besides contributions from the PNA strand. TMD reconstitution of oligomers **15** and **16** in lipid bilayers with a bilayer spanning orientation was proven via analysis of intrinsic tryptophan fluorescence (Supporting Information) and more importantly, in-house as well as anomalous X-ray scattering experiments.[52,53] The tryptophan fluorescence was monitored for peptides inserted into LUVs composed of DLPC at a peptide-to-lipid (P/L) ratio of 1/600. A hypsochromic shift of the tryptophan fluorescence relative to that of tryptophan in aqueous solution ($\lambda_{max,em}$ = 350 nm) indicated the tryptophan residues to be located in a more hydrophobic environment.[54,55] The maximum of the fluorescence emission band was located at 336 nm for peptide **15** and at 338 nm in case of the equimolar mixture of peptides **15** and **16**. This is in line with the preference of tryptophan to be located at the bilayer−water interface.[56−60]

(50) Stafforst, T.; Diederichsen, U. *Eur. J. Org. Chem.* **2007**, 681–688.
(51) Koch, T.; Hansen, H. F.; Andersen, P.; Larsen, T.; Batz, H. G.; Otteson, K.; Økrum, H. *J. Pept. Res.* **1997**, 80–88.
(52) Khattari, Z.; Brotons, G.; Arbely, E.; Arkin, I. T.; Metzger, T. H.; Salditt, T. *Physica B* **2006**, *86*, 1521–1531.
(53) Schneggenburger, P. E. Unpublished results, 2010.
(54) Ren, J.; Lew, S.; Wang, J.; London, E. *Biochemistry* **1999**, *38*, 5905–5912.
(55) Lew, S.; Ren, J.; London, E. *Biochemistry* **2000**, *39*, 9632–9640.
(56) Chattopadhyay, A.; Raghuraman, H. *Curr. Sci.* **2004**, *87*, 175–180.
(57) Bong, D. T.; Janshoff, A.; Steinem, C.; Ghadiri, M. R. *Biophys. J.* **2000**, *78*, 839–845.
(58) Strandberg, E.; Morein, S.; Rijkers, D. T. S.; Van der Wel, P. C. A.; Liskamp, R. M. J.; Killian, J. A. *Biochemistry* **2002**, *41*, 7190–7198.
(59) De Planque, M. R. R.; Boots, J.-W. P.; Rijkers, D. T. S.; Liskamp, R. M. J.; Greathouse, D. V.; Killian, J. A. *Biochemistry* **2002**, *41*, 8396–8404.
(60) De Planque, M. R. R.; Demmers, J. A. A.; Bonev, B. B.; Koeppe II, R. E.; Greathouse, D. V.; Separovic, F.; Watts, A.; Killian, J. A. *Biochemistry* **2003**, *42*, 5341–5348.

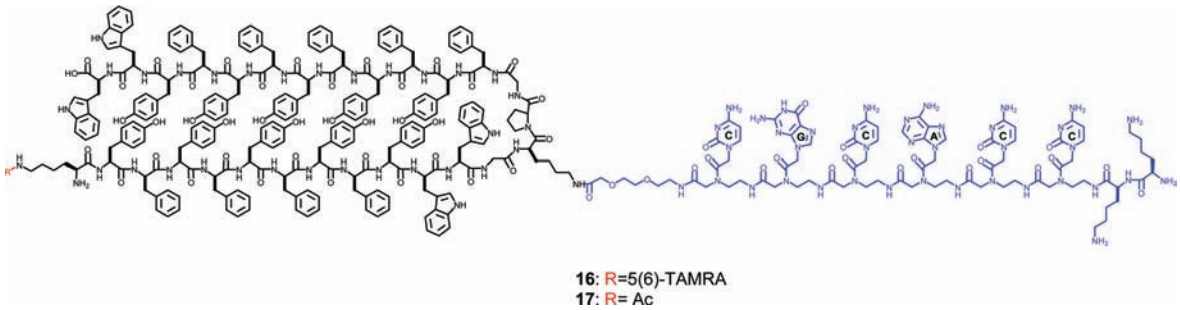

Figure 4. Molecular representation of the acceptor labeled and nonlabeled constructs.

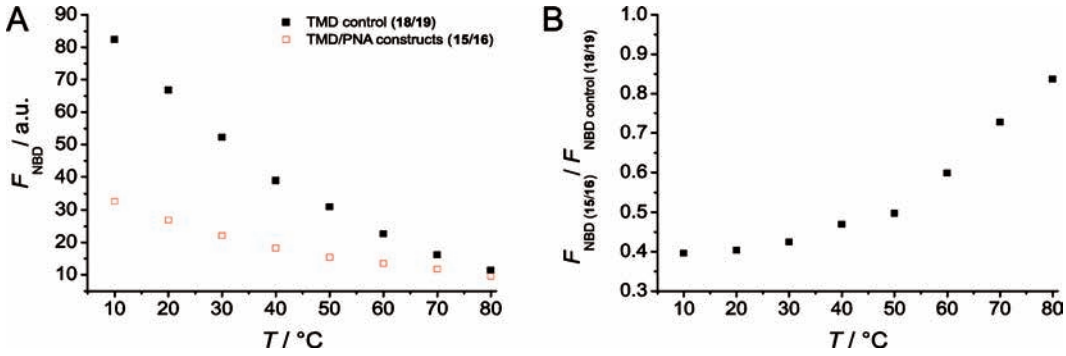

Figure 5. Temperature dependent FRET experiment in DLPC-LUVs. (A) The NBD-fluorescence emission at 538 nm is displayed as a function of temperature for the equimolar mixture of the control species **18** (NBD)/**19** (TAMRA) lacking the PNA recognition moieties (black data points) and the equimolar mixture of the PNA/TMD constructs **15** (NBD)/**16** (TAMRA) (red data points). The experiments were performed at a total peptide concentration of 5.5 μM and a P/L-ratio of 1/600. (B) Ratio of the donor fluorescence of peptides **15**/**16** and peptides **18**/**19** as a function of temperature.

Temperature Controlled Recognition of Peptide Helices in Lipid Vesicles. Besides analytical ultracentrifugation,[4,61−63] chromatographic,[4] and spectroscopic methods,[62] FRET experiments have been successfully applied to evaluate the oligomeric state of peptides not only in a micellar environment,[63] but also within lipid bilayers.[25−27,64] For instance, several variants of the GCN4 (leucine zipper) motif have been independently studied by the above-mentioned methods giving essentially the same results.[25,26,61−63] Since dynamic interactions of an entire molecular ensemble are in the scope of the presented study focusing on switching between two oligomerization states, a detergent-free setup was favored.[24−28] Therefore, we made use of FRET between the donor (NBD) and acceptor (TAMRA) labeled TMD/PNA constructs **15** and **16** to elucidate aggregate formation of the TMD peptides within large unilamellar DLPC vesicles by molecular recognition of the PNAs outside the membrane.

It is expected that a change in temperature affects the aggregation of the TMD peptides as a result of pairing or melting of the PNA double strands. To prove this hypothesis, temperature dependent FRET-experiments were performed. First, the fluorophore-labeled species (H-(K(NBD)Y(FY)$_4$WW-GK(Ac)PG-(FY)$_5$WW-OH (**18**) and H-(K(TAMRA)Y(FY)$_4$WW-GK(Ac)PG-(FY)$_5$WW-OH (**19**), both lacking the PNA recognition unit, were inserted into DLPC vesicles at an equimolar ratio and the donor fluorescence intensity was recorded at 538 nm. The donor fluorescence intensity decays with increasing temperature (Figure 5A), which is attributed to an increase in statistical quenching at elevated temperature and by a decrease in the NBD quantum yield with increasing temperature.[65] If, however, the PNAs containing TMD peptides **15** and **16** are present in the vesicles, the donor fluorescence intensity is considerably smaller at low temperature (Figure 5A) than for the PNA lacking TMD peptides **18** and **19**. The low donor fluorescence can be explained by an efficient energy transfer to the acceptor. For vesicles containing equimolar concentrations of **15** and **16**, the decrease in donor fluorescence upon increasing the temperature is less pronounced and shows a change in slope between 40 and 50 °C, which is more easily observed in Figure 5B, where $F_{\mathrm{NBD(15/16)}}/F_{\mathrm{NBD(18/19)}}$ is plotted. This change in slope is a result of a partial recovery of the donor fluorescence at elevated temperature consistent with the notion that the donor−acceptor distance increases. Comparing the temperature dependence with the melting curve of pure PNAs **9**/**10** (see Figure 3), this observation can be assigned to a melting of the PNA double strands followed by a dissociation of the TMD peptides. A contribution from a lipid phase transition can be ruled out (t_{m} (DLPC) = −2.1 °C).

Base pair recognition of the PNA strands is supposed to result in dimeric TMD/PNA assemblies. The oligomerization state can be assessed by variation of the acceptor-peptide fraction (χ_{A})[26] at a constant total peptide concentration (Figure 6). Compound **17** with the acylated lysine side chain instead of the attached fluorescence label was used to replace the TAMRA-labeled

(61) Gratkowski, H.; Lear, J. D.; DeGrado, W. F. *Proc. Natl. Acad. Sci. U.S.A.* **2001**, *98*, 880–885.
(62) Gratkowski, H.; Dai, Q.-h.; Wand, A. J.; DeGrado, W. F.; Lear, J. D. *Biophys. J.* **2002**, *83*, 1613–1649.
(63) Lear, J. D.; Stouffer, A. L.; Gratkowski, H.; Nanda, V.; DeGrado, W. F. *Biophys. J.* **2004**, *87*, 3421–3429.
(64) Merzlyakov, M.; You, M.; Li, E.; Hristova, K. *J. Mol. Biol.* **2006**, *358*, 1–7.
(65) Fleming, K. G. *J. Mol. Biol.* **2002**, *323*, 563–571.

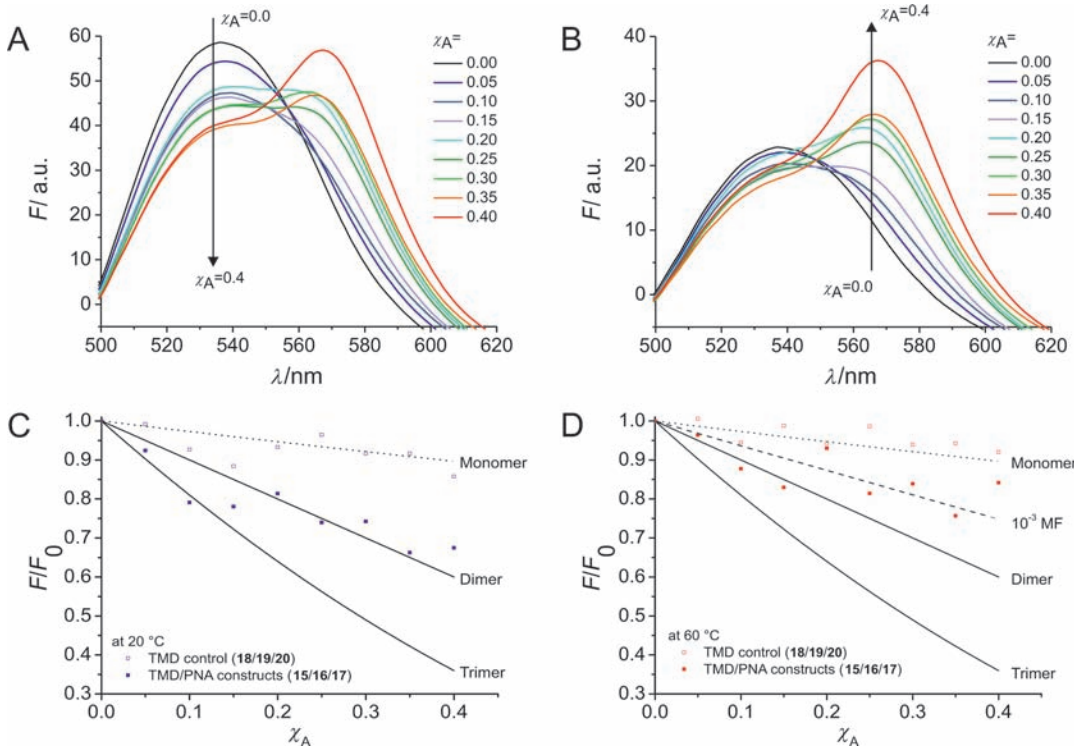

Figure 6. (A and B) Fluorescence emission spectra of the NBD-donor labeled compound **15** (2.75 μM) with a maximum at 537 nm and varying amounts of the acceptor species **16** (from $\chi_A = 0.00$ to $\chi_A = 0.40$) with a maximum at 571 nm recorded at 20 °C (A) and 60 °C (B). The nonlabeled compound **17** was added at various amounts to yield a total peptide concentration of 5.5 μM and a P/L ratio of 1/1000. (C and D) Plots of the relative changes in NBD-fluorescence emission as a function of χ_A for the TMD/PNA (**15**/**16**/**17**) and TMD control peptides (**18**/**19**/**20**) at (C) 20 °C and (D) 60 °C. The black lines are calculated plots based on the assumption of peptide monomers (dotted line), dimers, trimers (solid lines) or a monomer−dimer equilibrium (dashed line) with a dissociation constant given in mole fractions (MF).

peptide **16**, thus, keeping the P/L-ratio constant. The fluorescence emission spectra at $T < T_m$ ($T = 20$ °C) show a decrease in donor fluorescence, while the acceptor fluorescence increases with higher concentration of the acceptor species **16** (Figure 6A) indicating the occurrence of a FRET process. The ratio between maximum donor and acceptor fluorescence is different at 20 and 60 °C (Figure 6A,B), which might be a result of the different temperature dependencies of the NBD and TAMRA extinction coefficients. However, this is canceled out as only relative changes of the fluorescence intensity are plotted. A plot of the relative fluorescence F/F_0 (χ_A) of the NBD-labeled donor peptides, with F_0 being the fluorescence of the acceptor-free sample, shows an increased quenching of the NBD-fluorescence with increasing acceptor concentration. To evaluate the data and elucidate which aggregates might have been formed as a function of temperature, several scenarios are discussed: (i) Assuming that only peptide monomers are present in the vesicles, statistical occurrence of FRET due to the presence of several acceptors in any given vesicle has to be taken into consideration. With a Förster radius of $R_0 = 5.1$ nm (see theoretical treatment of the FRET data),[26] the plots shown in Figure 6C,D (black dotted lines, monomer) are calculated. For peptides lacking the PNA sequences (**18**, **19**, and **20**: H-(K(Ac)Y(FY)$_4$WW-GK(Ac)PG-(FY)$_5$WW-OH), the calculated plot is slightly above the data points obtained at 20 °C (Figure 6C), which is probably just a result of the variance of the data points. The calculated plot is in very good agreement with the data points at 60 °C (Figure 6D). This demonstrates that all peptides are in the monomeric state at 60 °C, while at 20 °C, one can state that the majority is monomeric. (ii) Assuming a binomial distribution of donors and acceptors in a dimeric assembly as a result of base pair recognition results in the plots shown in Figure 6C,D with a significantly larger slope (black solid lines, dimer). The calculated curve is in rather good accordance with the data points obtained for the TMD/PNA construct (**15**/**16**/**17**) at 20 °C but does not fit the data well at 60 °C. This lets us assume that the TMD/PNA construct is almost completely assembled in a dimeric fashion at 20 °C, while it is neither purely monomeric nor dimeric at 60 °C. (iii) It is more likely that instead of stable dimers, a monomer−dimer equilibrium of the TMD/PNA construct is established at 60 °C.

A curve assuming a monomer−dimer equilibrium with a dissociation constant of 10^{-3} MF was calculated, shown in Figure 6D (black dashed line), which follows the same trend as the data points.[28,26] (iv) To rule out that even larger aggregates are formed, we also calculated plots of F/F_0 (χ_A) for the formation of trimers (Figure 6C,D, black solid lines, trimer). It is obvious that a considerable larger change of F/F_0 is expected, which could not be found in the experiments.

From the overall results, we conclude that the degree of association/dimer formation is a function of base pair recognition in the aqueous phase, which is temperature dependent. While at 20 °C, the data points reveal that a majority of TMD/PNA peptides are in the dimeric state, clear monomer−dimer equilibrium is established at 60 °C. Apparently, a complete dissociation of the dimer assembly is not achieved even at a temperature well above the melting temperature of the PNA double strand **9**/**10** lacking the transmembrane domain. It is very likely that the lipid bilayer itself influences the TMD association. Furthermore, the transmembrane helix aggregation might con-

tribute to the overall stability, since aggregation was also observed during chromatographic purification of various TMD constructs.

Conclusion

The rational design of a peptide motif providing a transmembrane part and a PNA unit for specific recognition was introduced to study helix−helix interactions within lipid bilayer structures at the membrane−water interface. Different constructs with respect to labeling and recognition sequences were assembled by means of SPPS in combination with orthogonal fluorophore and linker functionalization. A peptide hairpin with a stable $\beta^{5.6}$-double helical conformation derived from a D,L-alternating gramicidin A analogue served as membrane spanning domain. In combination with the attached PNA recognition unit, dimerization of these TMD/PNA constructs was observed in large unilamellar DLPC-vesicles. Monitoring of dimer−monomer equilibrium was feasible by temperature and concentration dependent FRET analysis of NBD and TAMRA labeled species that revealed a dimeric assembly at 20 °C and a fractional depairing at elevated temperature providing a smaller dissociation constant.

The novel TMD/PNA conjugate composes the first synthesis of a membrane associated peptide model system that uses distinct recognition at the membrane outside to study the in-membrane dimer-formation of structured domains that are spanning the entire lipid bilayer core. With such a model, it is possible to investigate the dependency of the above-described, native recognition/assembly process from various, especially lipid bilayer related parameters. These are, for example, hydrophobic matching, interfacial anchoring, and lipid domain formation. Up to now, such properties were merely studied with respect to a direct interaction within the hydrophobic membrane core.[3,10] Since cellular key functions are driven by this poorly understood mechanism, the application of the novel peptide model and its variants will enable a learning process about the dynamics, organization, and geometrical preferences of membrane bound species and, therefore, provide insight into the biophysical demands that have to be fulfilled to exhibit biochemical functioning.

The respective constructs, possibly equipped with modified recognition units, will allow for more extensive, reliable dimer−monomer switching. The potential fusogenicity of the constructs and expansion of the outer-membrane recognition unit leading to higher organized transmembrane domains such as pore assemblies is also in the scope of future work. This could be achieved by promoting the formation of PNA triple helices by sequence selection or by applying guanine tetrad assemblies.[20,21,49]

Acknowledgment. Generous support of the Deutsche Forschungsgemeinschaft (SFB 803) is gratefully acknowledged. P.E.S. is grateful for a doctoral bridging stipend of the Göttingen Graduate School for Neuroscience and Molecular Biosciences (GGNB). We dedicate this paper to Professor Horst Kessler on the occasion of his 70th birthday.

Supporting Information Available: Materials and methods, peptide/PNA synthesis and purification, notes on purification, analytical data, CD and UV spectroscopic methods, fluorescence spectra. This material is available free of charge via the Internet at http://pubs.acs.org.

JA1006349